



3-Aminobenzamide Prevents Concanavalin A-Induced Acute Hepatitis by an Anti-inflammatory and Anti-oxidative Mechanism

Joram Wardi¹ · Orna Ernst^{2,3} · Anna Lilja² · Hussein Aeed¹ · Sebastián Katz² · Idan Ben-Nachum² · Iris Ben-Dror² · Dolev Katz² · Olga Bernadsky⁴ · Rajendar Kandhikonda⁵ · Yona Avni¹ · Iain D. C. Fraser³ · Roy Weinstein⁵ · Alexander Biro⁶ · Tsaffir Zor²

Received: 21 November 2017 / Accepted: 24 August 2018
© Springer Science+Business Media, LLC, part of Springer Nature 2018

Abstract

Background and Aims Concanavalin A is known to activate T cells and to cause liver injury and hepatitis, mediated in part by secretion of TNF α from macrophages. Poly(ADP-ribose) polymerase-1 (PARP-1) inhibitors have been shown to prevent tissue damage in various animal models of inflammation. The objectives of this study were to evaluate the efficacy and mechanism of the PARP-1 inhibitor 3-aminobenzamide (3-AB) in preventing concanavalin A-induced liver damage.

Methods We tested the *in vivo* effects of 3-AB on concanavalin A-treated mice, its effects on lipopolysaccharide (LPS)-stimulated macrophages in culture, and its ability to act as a scavenger in *in vitro* assays.

Results 3-AB markedly reduced inflammation, oxidative stress, and liver tissue damage in concanavalin A-treated mice. In LPS-stimulated RAW264.7 macrophages, 3-AB inhibited NF κ B transcriptional activity and subsequent expression of TNF α and iNOS and blocked NO production. *In vitro*, 3-AB acted as a hydrogen peroxide scavenger. The ROS scavenger *N*-acetylcysteine (NAC) and the ROS formation inhibitor diphenyleneiodonium (DPI) also inhibited TNF α expression in stimulated macrophages, but unlike 3-AB, NAC and DPI were unable to abolish NF κ B activity. PARP-1 knockout failed to affect NF κ B and TNF α suppression by 3-AB in stimulated macrophages.

Conclusions Our results suggest that 3-AB has a therapeutic effect on concanavalin A-induced liver injury by inhibiting expression of the key pro-inflammatory cytokine TNF α , via PARP-1-independent NF κ B suppression and via an NF κ B-independent anti-oxidative mechanism.

Keywords Liver failure · Inflammation · Macrophages · TNF α · Reactive oxygen species · NF κ B

Abbreviations

3-AB	3-Aminobenzamide	IFN γ	Interferon γ
ALT	Alanine aminotransferase	LPS	Lipopolysaccharide
AST	Aspartate aminotransferase	MDH	Malate dehydrogenase
ConA	Concanavalin A	NAC	<i>N</i> -acetylcysteine
DPI	Diphenyleneiodonium	NF κ B	Nuclear factor kappa B
HRP	Horseradish peroxidase	NO	Nitric oxide
		Nox	NADPH oxidase
		PARP-1	Poly(ADP-ribose) polymerase-1
		PF2	Peroxyfluor-2
		ROS	Reactive oxygen species
		SOD	Superoxide dismutase
		TNF α	Tumor necrosis factor α

Joram Wardi and Orna Ernst have contributed equally to this article.

- ✉ Joram Wardi
joram831@gmail.com
- ✉ Alexander Biro
abiro@wolfson.health.gov.il
- ✉ Tsaffir Zor
tsaffyz@tauex.tau.ac.il

Extended author information available on the last page of the article

Introduction

Acute liver injury by viruses, toxins, drugs, or autoimmune mechanisms may lead to fulminant hepatitis and liver failure. Available medications are limited and additional agents are needed. The T cell mitogen, concanavalin A (ConA), induces acute hepatitis in a well-known experimental mouse model of liver injury. Various immune cells are involved in the resulting inflammation, including CD4⁺ T cells [1], natural killer T (NKT) cells [2], and macrophages [3]. ConA-stimulated T cells release low amounts of interferon (IFN) γ and tumor necrosis factor (TNF) α [4, 5]. Importantly, a T cell-secreted factor activates the resident macrophages (Kupffer cells) and infiltrating monocytes-derived macrophages to express and release high levels of the key pro-inflammatory cytokine TNF α [4], in part via the transcription factor NF κ B [6]. In turn, the stimulated macrophages synergistically amplify IFN γ expression by ConA-stimulated T cells, hence establishing a reciprocal cross talk [4]. Inflammation and liver damage in various mouse models were considerably reduced in TLR4-deficient mice, implicating also TLR4 in macrophages activation [7–9]. The activation of TLR4 may be carried out by endogenous proteins, such as extracellular histones and high-mobility group box 1 (HMGB1), which are released from liver cells following ConA treatment and are essential for hepatitis development [9, 10]. Thus, liver macrophages and the TNF α they express are instrumental for development of inflammation and liver damage in response to toxins, including ConA [3], and TLR4 activation is essential for this process [10].

Poly(ADP-ribose) polymerase-1 (PARP-1) is a DNA repair enzyme that is activated in acute cellular injury. It binds to DNA breaks and uses NAD⁺ as a substrate to catalyze poly-ADP-ribosylation on itself and on other target proteins to enable recruitment of repair proteins to the damaged DNA. Yet, excessive PARP-1 activity results in NAD⁺ and ATP depletion and cell necrosis [11]. PARP-1 was also found to be involved in other cellular processes. For example, PARP-1 activation in immune cells results in posttranslational modification of NF κ B p65 [12] and subsequent expression of pro-inflammatory cytokines, such as TNF α [13]. Accordingly, PARP-1 inhibition or knockout decreased tissue damage in various animal models of inflammation and ischemia–reperfusion injury [14]. Inhibition of PARP-1 attenuated liver injury in the models of bile duct ligation and carbon tetrachloride (CCl₄) [15], acetaminophen overdose [16] and alcoholic liver disease [17]. The present study examined the preventive and therapeutic effects of the PARP-1 inhibitor 3-aminobenzamide (3-AB) in an acute immune model of ConA-induced experimental hepatitis in mice. The mechanism of action of 3-AB was further studied using stimulated macrophages and in vitro assays.

Materials and Methods

Reagents

Lipopolysaccharide (LPS; Escherichia coli serotype O55:B5), concanavalin A (ConA), 3-aminobenzamide (3-AB), Tween-20, isoproterenol, 3-isobutyl-1-methylxanthine (IBMX), NADPH, cytochrome C, *N*-acetylcysteine (NAC) and DPI were purchased from Sigma-Aldrich (St. Louis, MO). The antibodies against p65 NF κ B phosphorylated on Ser-536 or Ser-276 were purchased from Cell Signaling Technology (Danvers, MA). The antibodies against general p65 NF κ B, α -tubulin, iNOS, and PARP-1 were purchased from Merck (Burlington, MA), Santa Cruz Biotechnology (Santa Cruz, CA), Abcam (Cambridge, UK), and Alexis (San Diego, CA), respectively. Infrared dye-labeled secondary antibodies and blocking buffer were obtained from Li-COR Biosciences (Lincoln, NE). Hoechst 33342 and Alexa Fluor 488-conjugated secondary antibody were from Thermo Fisher Scientific (Waltham, MA). Paraformaldehyde was from Electron Microscopy Sciences (Hatfield, PA). XTT, L-glutamine, and penicillin–streptomycin–nystatin were purchased from Biological Industries (Beit Haemek, Israel). DMEM, OptiMEM, and FBS were purchased from GIBCO. The TNF α ELISA set that included also the horseradish peroxidase (HRP) used for the H₂O₂ assay was purchased from R&D Systems (Minneapolis, MN). The HRP substrate mix (TMB and H₂O₂) and LiDS were purchased from Merck KGaA (Darmstadt, Germany). The mouse TNF α promoter luciferase reporter gene construct was a kind gift from Dr. C. Yu (Xiamen University, Xiamen, Fujian, China) [18]. A plasmid carrying four copies of the consensus NF κ B binding site upstream to a luciferase reporter gene was purchased from Clontech (Mountain View, CA). A CRE-containing EVX-1 promoter luciferase reporter gene construct (hereafter CRE-luciferase, [19]) was a kind gift from Dr. M. Montminy (Salk Institute, La-Jolla, CA). A plasmid carrying five copies of the AP-1 binding site from the human collagenase promoter upstream to a luciferase reporter gene (hereafter AP-1-luciferase, [20]) was a kind gift from Dr. P. Angel (German Cancer Research Center, Heidelberg, Germany). Plasmids were amplified using DH10B bacteria (Invitrogen, Carlsbad, CA) and purified using Endofree Plasmid Maxi Kit (Qiagen, Hamburg, Germany). TransIT-2020 and Lipofectamine 2000 transfection reagents were purchased from Mirus Bio (Madison, WI) and Invitrogen (Carlsbad, CA), respectively. The Cell Nucleofector kit V was purchased from Lonza (Basel, Switzerland). The Dual-luciferase reporter assay kit and the Griess reagent were from Promega (Fitchburg, WI). The siRNA targeting PARP-1 and a non-specific control were from Dharmacon (Lafayette CO). The gRNA oligonucleotides were from IDT (Skokie,

IL), and the pX330-U6-Chimeric_BB-CBh-hSpCas9 vector was a gift from Feng Zhang (Addgene plasmid # 42230). The complete protease inhibitors mixture was purchased from Roche (Mannheim, Germany).

Animal Care

Male Balb/c (8–10 weeks old) mice, obtained from Tel-Aviv University animal breeding center, were kept in the animal breeding house of the Wolfson Medical Center and fed a Purina chow ad libitum. The animals were kept with a 12-h light–dark cycle at constant temperature and humidity.

Cell Culture

Mouse RAW264.7 macrophage cells and mouse EL-4 T cells were obtained from American Type Culture Collection (ATCC, Rockville, MD) and were routinely verified to be mycoplasma-free. The cells were grown to 80–90% confluence in DMEM medium supplemented with 100 U/ml penicillin, 100 µg/ml streptomycin, 1250 U/ml nystatin, and L-glutamine to a final concentration of 12 mM (hereafter culture medium), and with 10% FBS, at 37 °C in a humidified incubator with 5% CO₂.

In vivo Experiments

Experimental hepatitis was induced as previously described [21], by injecting ConA (10 mg/kg) into the tail vein of the mice ($n = 4$ –12/group). NaCl (0.9%) served as vehicle. Two doses of the PARP-1 inhibitor 3-AB were administered intraperitoneally (i.p.) at 50 mg/kg—concurrently with the ConA intravenous (i.v.) injection and 2 h later. Blood was drawn at 2 h and 6 h for serum TNF α measurement and at killing time (24 h) for liver enzymes measurement. Oxidative stress was evaluated by malondialdehyde (MDA) measurements in the extracted liver tissues at killing. The livers were fixated in formalin and stained by hematoxylin–eosin.

In vitro TNF α Expression

RAW264.7 macrophages and EL-4 T cells were maintained for 48 h prior to the experiment in 96-well plates, at $1.0 \cdot 10^5$ cells per well, in culture medium supplemented with 5% FBS, up to a confluence of 90%. The culture medium was replaced 2 h before treatment in order to avoid the artifact of medium replacement on signaling. Macrophages and T cells were stimulated with either LPS (100 ng/ml) or with ConA (25 µg/ml), respectively, in the presence or absence of 3-AB (20 mM unless indicated otherwise) at 37 °C for the indicated incubation time (2–24 h).

TNF α Assay

TNF α secretion to the medium was measured with a commercially available ELISA reagents set, according to the manufacturer's instructions, using a microplate reader (Bio-Tek, Winooski, Vermont). TNF α secretion was undetectable (< 20 pg/ml) in resting cells.

Serum Liver Enzymes Analysis

The degree of liver injury was evaluated by measuring serum levels of the liver enzymes alanine aminotransferase (ALT) and aspartate aminotransferase (AST) using a COBAS 8000 analyzer (Roche Diagnostics, Madison, WI), according to the manufacturer's instructions. Briefly, enzymatic activities of serum ALT and AST were determined by measurement of NADH consumption in a follow-up reaction with lactate dehydrogenase (LDH) or malate dehydrogenase (MDH), respectively.

Malondialdehyde (MDA) Analysis

Mice livers were frozen with liquid nitrogen and stored at – 70 °C until assayed for MDA. Liver tissue (5 g) was cut into small pieces using a razor blade and homogenized in DDW (1:10 w/v). Liver homogenate was centrifuged at 900 rpm for 5 min, and then, the supernatant was collected and centrifuged at 20,000 rpm for 30 min. MDA in the clear supernatant was measured and expressed as nmol/g wet tissue using the thiobarbituric acid method [22].

Histology

Following mice killing, the livers were removed and randomly sectioned and processed for light microscopy. The specimens were fixed with 5% neutral formalin solution and embedded in paraffin. Sections of 5 µm were made and then stained with hematoxylin and eosin and Masson trichrome. The liver tissue slices were scanned and scored for inflammation and necrosis by a grading scale of 0–3 as previously described [23].

Transfection and Reporter Gene Assay

RAW264.7 macrophages were grown for 24 h at 2×10^5 cells per well (24-well plates) in culture medium supplemented with 10% FBS. The cells were then transfected for 24 h with 0.2 µg of the indicated reporter plasmid and 0.07 µg of TK-Renilla luciferase (for normalization). The plasmids were initially incubated with TransIT-2020 transfection reagent in OptiMEM for 15 min at RT. Following transfection, the cells were washed and stimulated with LPS (100 ng/ml) in the presence or absence of 3-AB or ROS inhibitors, at

37 °C for the indicated time, after which luciferase activity in cell extracts was determined following the manufacturer's instructions. Data were expressed as a ratio of firefly luciferase activity divided by the Renilla luciferase activity.

PARP-1 Silencing Using siRNA

RAW264.7 macrophages were grown for 24 h in 24-well plates, at 1.2×10^5 cells per well, in culture medium supplemented with 10% FBS. Transfection with siRNA against PARP-1 (or a non-specific control sequence) was performed as described by Fraser et al. [24]. A mixture of each siRNA with Lipofectamine 2000 transfection reagent, initially incubated in OptiMEM medium for 20 min at room temperature, was added to the cells at 100 nM for the first 4 h, after which the volume was increased so the siRNA was at a concentration of 62.5 nM for the following 20 h. The cells were washed and the transfection process was repeated the next day for another 24 h. The siRNA-containing medium was removed, and the cells were seeded for a recovery period of 24 h in a 96-wells plate (2×10^5 cells per well, for TNF α assay) and a 24-wells plate (5×10^5 cells per well, for PARP-1 expression analysis by WB). For the TNF α assay, the cells were pre-incubated with 3-AB (20 mM) or vehicle for 2 h, and then, LPS (100 ng/ml) was added for 24 h at 37 °C. TNF α secretion was analyzed by ELISA.

Generation of PARP-1 Knockout Cells

The KO cells were prepared as described by Zhang et al. [25]. In short, the gRNA (forward sequence CGAGTGGAG TACGCGAAGAG) was designed using the MIT website (crispr.mit.edu) and incorporated into a pX330-U6-Chimeric_BB-CBh-hSpCas9 vector [26]. The plasmid was purified using the Endofree Plasmid Maxi Kit and electroporated into RAW264.7 cells using Cell Nucleofector kit V. Positively transfected cells were sorted by FACS, and single-cell clones were analyzed by western blot. Mock cells were created by transfection with a plasmid not containing gRNA and sorting.

Analysis of p65 NF κ B Phosphorylation on Ser-536

RAW264.7 macrophages were grown for 48 h at 2×10^5 cells per well (24-well plate) in culture media supplemented with 10% FBS. The cells were washed and stimulated with LPS (100 ng/ml) in the presence or absence of 3-AB (20 mM) at 37 °C for 30 min. The cells were then washed with ice-cold PBS, and whole-cell lysates were prepared using RIPA buffer (pH 7.5, 20 mM Tris-HCl, 20 mM sodium phosphate buffer, 150 mM NaCl, 1% Triton X-100, 0.5% deoxycholate, 0.1% SDS, 5 mM EDTA, 3 mM EGTA, 1 mM sodium orthovanadate, 10 mM sodium fluoride, 10 mM sodium

pyrophosphate, 3 mM β -glycerophosphate, complete protease inhibitors mixture). The lysates were centrifuged at $20,000 \times g$ for 20 min at 4 °C, and the supernatants were stored at -80 °C until analysis by western blot.

Western Blotting

Cell extracts (30–50 μ g protein) were boiled for 5 min in SDS-PAGE buffer, subjected to 10% SDS-PAGE, and proteins were transferred to Immobilon-FL polyvinylidene fluoride (PVDF) membrane. The membrane was simultaneously exposed to antibodies against iNOS (1:400 dilution) or PARP-1 (1:4000 dilution) and α -tubulin (1:1000 dilution) for normalization, or to an antibody against phosphorylated Ser-536 p65 NF κ B (1:1000 dilution) and general p65 NF κ B (1:500 dilution) for normalization. Exposure to dye-labeled secondary antibodies (1:10,000 dilution) then followed. Two-color imaging and quantitative analysis of western blots was performed using the Odyssey infrared imaging system (Li-COR Biosciences), according to the manufacturer's instructions.

Fluorescence Microscopy—Analysis of p65 NF κ B Phosphorylation on Ser-276 and Nuclear Translocation

The time course of p65 NF κ B phosphorylation on Ser-276 and nuclear translocation was determined as previously described [27]. In brief, 1×10^4 RAW264.7 cells per well were seeded in a black, clear bottom 96-well plate. The cells were pre-treated with or without 3-AB (20 mM) for 2 h before addition of LPS (100 ng/ml) for the indicated time. At the end of the experiment, cells were fixed using 4% paraformaldehyde for 10 min and then blocked and permeabilized using 5% BSA and 0.05% Tween 20 for 1 h. Staining was performed with Hoechst 33342, anti-phospho-Ser-276 p65 NF κ B (1:500 dilution), and Alexa Fluor 488 conjugated secondary antibody (1:1000 dilution). Imaging and quantitation of nuclear phospho-p65 was performed on 500 cells/well using the Cellinsight NXT high content imager (Thermo Scientific).

Nitric Oxide (NO) Analysis

NO was measured using the Griess method according to the manufacturer's instructions.

Superoxide Assay

Superoxide production rate was measured as previously described [28]. In short, the cell-free assay of NADPH oxidase (Nox) activity is setup by reconstitution of the recombinant cytosolic subunits p47^{phox}, p67^{phox}, and the small

GTPase Rac1 (100 nM each) with membrane liposomes containing the catalytic cytochrome b_{558} component (5 nM). The reaction mixture contains lithium dodecyl sulfate (LiDS, 0.12 mM) and cytochrome C (0.2 mM) which is specifically reduced by superoxide. The reaction is started by the addition of NADPH (240 μ M) that reduces oxygen to form superoxide which in turn reduces cytochrome C leading to its increased absorbance at 550 nm, followed every 6 s over a period of 5 min. The inhibitors tested were 3-AB (10 mM), NAC (20 mM), and DPI (10 μ M). Specificity of cytochrome C reduction by superoxide was confirmed by superoxide dismutase (SOD, 250 u/ml) which enzymatically eliminates superoxide.

Hydrogen Peroxide (H_2O_2) Measurement—Enzymatic Assay

H_2O_2 (0.11 mM) was mixed with 3-AB (1–20 mM), NAC (20 mM), DPI (10 μ M), or vehicle (5% DMSO) and with the HRP substrate TMB (65 μ M). The reaction was started by the addition of HRP (1:500 dilution of the enzyme in the ELISA reagents set), and following 1.5 min it was terminated and analyzed as for the TNF α ELISA assay.

H_2O_2 Measurement—Fluorescent Probe Assay

The specific H_2O_2 probe peroxyfluor-2 (PF2) was synthesized as previously described [29]. H_2O_2 (50 μ M) was mixed with PF2 (0.1 mM) and either 3-AB (0.5–20 mM), NAC (0.1–20 mM), DPI (10 μ M) or vehicle (10% DMSO). Fluorescence development (λ_{ex} = 480 nm, λ_{em} = 530 nm) was followed for 5 h, every 20 min. The final 8 time points served for calculation of H_2O_2 concentration, which was linear up to 50 μ M, according to the calibration curve.

Protein Determination

Protein was determined by a modification of the Bradford procedure, which yields linear results, increased sensitivity, and reduced detergent interference, as we have previously described [30, 31]. Bovine serum albumin served as standard.

Statistics

All experiments were performed at least twice on different days. Values are expressed as mean and standard deviation where n represents the number of mice or biological replicate in each group. The 2-tailed Mann–Whitney test was used for intergroup comparison. *P* values of less than 0.05 were considered significant, and they represent statistical significance of the 3-AB treatment (e.g., LPS + 3-AB vs.

LPS alone), unless depicted otherwise. EC_{50} values were calculated using the GraphPad Prism 5 software.

Results

PARP-1 Inhibitor 3-AB Markedly Reduces Serum Levels of Liver Enzymes and Attenuates Oxidative Stress in Mice Exposed to ConA

To test the hypothesis that the PARP-1 inhibitor 3-AB would prevent ConA-induced experimental hepatitis, 3-AB at a dose of 50 mg/kg or vehicle was i.p.-injected to BALB/c mice concurrently with, as well as 2 h following, i.v. injection of ConA. Liver inflammation and damage were assessed by measurement of serum levels of the liver proteins alanine aminotransferase (ALT) and aspartate aminotransferase (AST) and of the pro-inflammatory cytokine TNF α , by determination of liver tissue levels of the oxidative stress marker malondialdehyde (MDA) and by liver histology. Figure 1a shows that 3-AB decreased serum ALT and AST levels by 93% and 76%, respectively, as measured 24 h after ConA injection. MDA tissue levels, reflecting liver oxidative stress, were increased 3.5-fold after 24 h in the ConA-treated group compared to only 1.8-fold in the group treated by both ConA and 3-AB, demonstrating 67% inhibition by 3-AB (Fig. 1b).

3-AB Improves Liver Histology in ConA-Induced Hepatitis

Liver histology performed 24 h after ConA injection shows marked inflammatory infiltrate containing lymphocytes and numerous plasma cells and prominent interface hepatitis, as well as foci of geographic hepatocyte necrosis in mid-zonal areas of the liver lobules (Fig. 1c). In contrast, 3-AB efficiently prevented both of these apparent ConA-induced liver damages; the portal areas in the 3-AB-treated group demonstrate only patchy minute inflammation by a few lymphocytes and no identified necrosis (Fig. 1c). Histology of mice treated with 3-AB only (without exposure to ConA) shows a normal liver (Fig. 1c). The therapeutic benefit of 3-AB administration was quantitatively demonstrated by significantly reduced necrosis and inflammation scores - 0.4 each, compared to 2.2 and 1.7, respectively, in mice treated with ConA alone (Fig. 1d).

3-AB Reduces ConA-Induced Serum TNF α Levels

As an early sign of inflammation, serum TNF α levels were measured 2 h and 6 h following ConA administration. Figure 1e shows that 3-AB reduced ConA-stimulated serum TNF α level by 72–75% at both time points. To conclude the

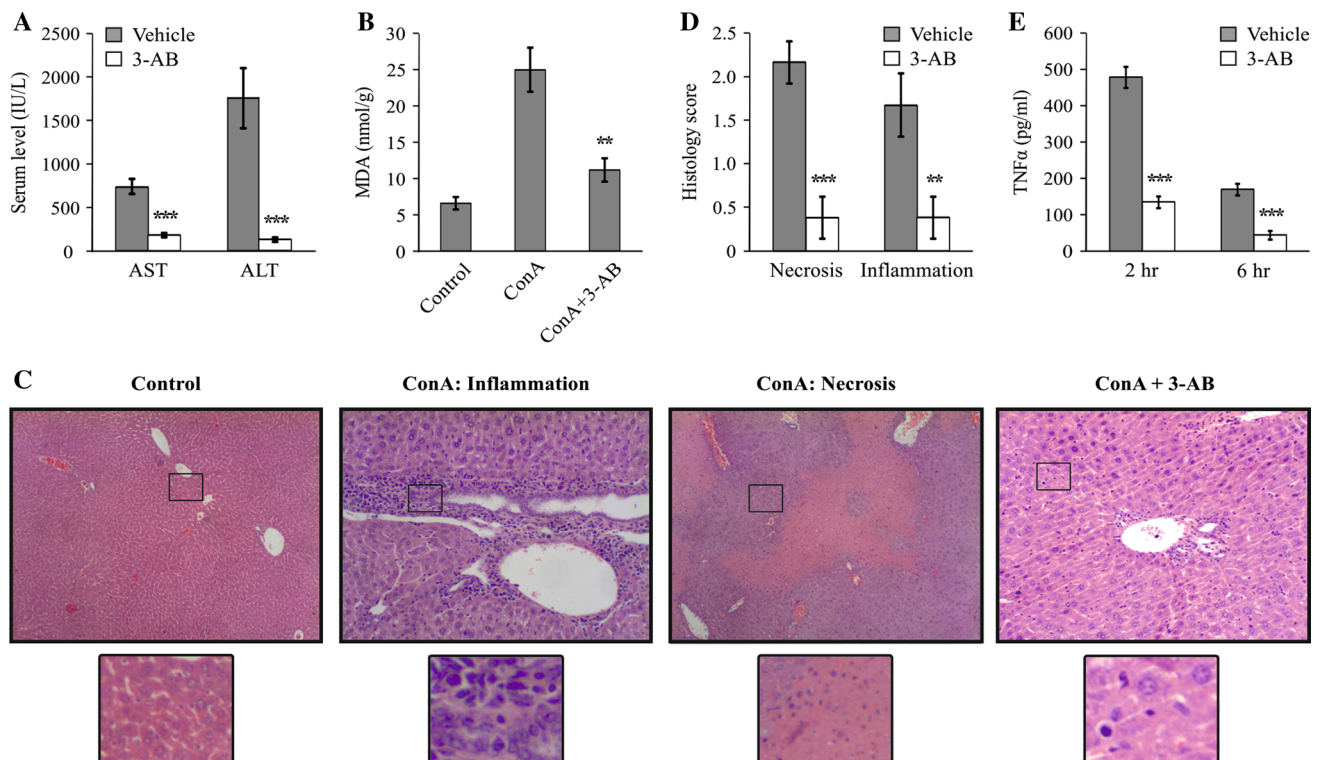


Fig. 1 3-AB protects against ConA-induced liver inflammation and damage. BALB/c mice were i.v.-injected with ConA (10 mg/kg, $t=0$) and i.p.-injected with two doses of 3-AB (50 mg/kg) at $t=0$ and at $t=2$ h. Liver damage (expressed as mean \pm SEM) was assessed by: **a** liver enzymes serum levels at $t=24$ h ($n=10$ – 12 /group); levels in the control (3-AB alone) group were 85 ± 17 and 53 ± 22 for AST and ALT, respectively. **b** Oxidative stress represented by MDA level in

liver tissue at $t=24$ h ($n=4$ – 8 /group); **c, d** liver histology at $t=24$ h (representative H&E staining; magnification 20 \times and 80 \times). Control mice were treated with 3-AB only. Histology shows a normal liver; **e** serum TNF α level at the indicated time points ($n=4$ – 10 /group). **a**–**e** * $p < 0.05$, ** $p < 0.01$ and *** $p < 0.001$ —relative to treatment with ConA alone. Levels in the control (3-AB alone) group were identical to naïve mice

in vivo experiment, 3-AB demonstrated a large therapeutic effect at all examined parameters in a mouse model of ConA-stimulated liver inflammation and damage.

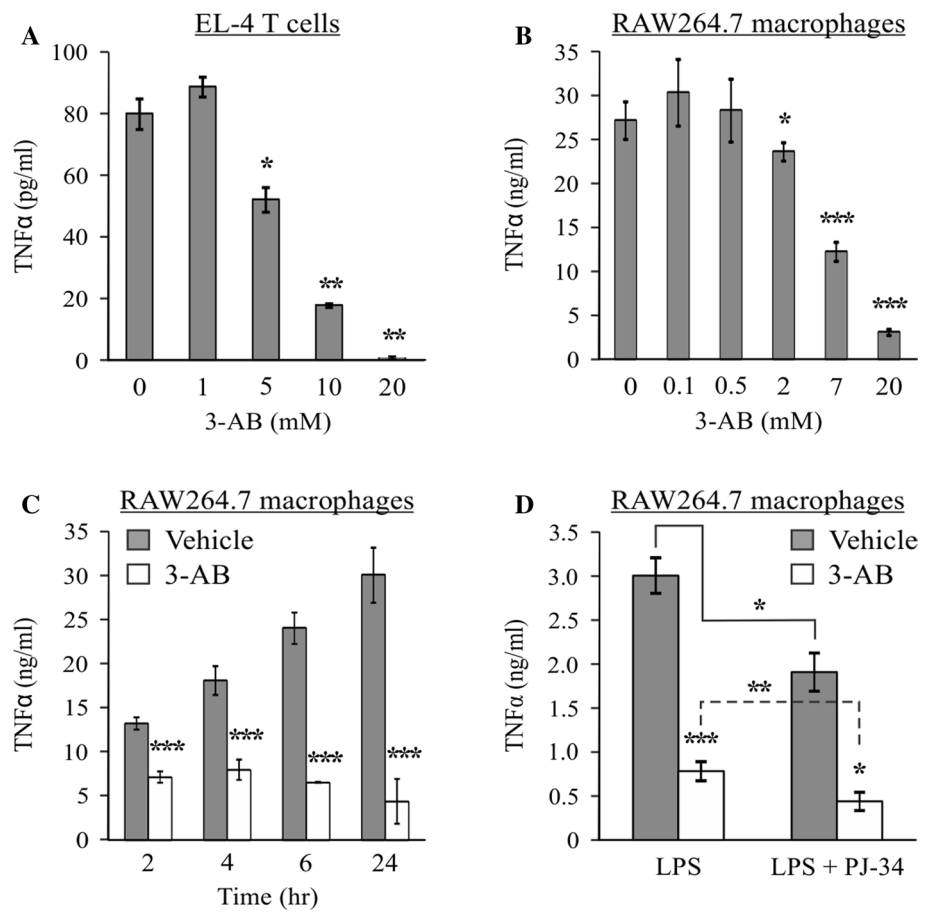
3-AB Inhibits TNF α Secretion from ConA-Stimulated T Cells and LPS-Stimulated Macrophages

As ConA directly targets T cells, we examined the in vitro effect of 3-AB on ConA-stimulated TNF α expression in cultured mouse T cells, EL-4. Figure 2 shows that 3-AB abolished TNF α secretion from EL-4 cells during a 24 h ConA incubation, with a maximal effect observed at a concentration of 20 mM and an EC₅₀ of 7 mM. Liver macrophages are accountable for the majority of the circulating [32] and intrahepatic [3] TNF α that is critical for the progression of hepatitis and liver damage induced by ConA. Moreover, ConA-stimulated T cells secrete factors that directly induce TNF α expression in macrophages [4]. Thus, we next sought to determine whether 3-AB can inhibit TNF α secretion not only from T cells, but also from macrophages. As TLR4 was demonstrated to be required for the development of liver damage in various mouse models [7], RAW264.7

macrophages were stimulated with the TLR4 agonist LPS in the presence or absence of 3-AB. As expected, following 24-h stimulation, the LPS-treated macrophages secreted three orders of magnitude more TNF α than the ConA-stimulated T cells (Fig. 2a, b). Importantly, 3-AB inhibited TNF α secretion from the LPS-stimulated RAW264.7 macrophages, with the same potency as in the T cell culture (EC₅₀=7 mM) (Fig. 2a, b). Thus, TNF α suppression by 3-AB appears to be independent of the context of cell type and stimulus. A time course experiment (Fig. 2c) demonstrated that the magnitude of the suppressive effect of 3-AB on LPS-stimulated TNF α secretion correlates with the co-incubation duration time, starting with 47% at 2 h and gradually increasing to 86% at 24 h. Cell viability was measured to confirm that 3-AB was not cytotoxic to the cells at the maximal time and concentration used in this study (data not shown).

We compared 3-AB with another PARP-1 inhibitor, PJ-34, in order to assess whether the effect on TNF α secretion should be attributed to PARP-1 inhibition. Interestingly, 3-AB inhibited LPS-stimulated TNF α secretion to a much larger extent than PJ-34 (75% vs. 37%, respectively). Moreover, 3-AB and PJ-34 additively inhibited LPS-stimulated

Fig. 2 3-AB inhibits TNF α secretion in stimulated T cells and macrophages. **a** Mouse EL-4 T cells were pre-incubated with 3-AB (0–20 mM) for 2 h and then ConA (25 μ g/ml) was added for 24 h; **b** RAW264.7 macrophages were pre-incubated with 3-AB (0–20 mM) for 2 h and then LPS (100 ng/ml) was added for 24 h; **c** RAW264.7 macrophages were pre-incubated with 3-AB (20 mM) or vehicle for 2 h and then LPS (100 ng/ml) was added for the indicated time; **d** RAW264.7 macrophages were pre-incubated with 3-AB (20 mM) and/or PJ-34 (10 μ M) for 2 h and then LPS (100 ng/ml) was added for 4 h; **a–d** TNF α secretion to the medium was measured by ELISA. Data represent mean \pm SD ($n=6$). * $p < 0.05$, ** $p < 0.01$, *** $p < 0.001$. TNF α was undetectable in resting cells



TNF α secretion, as 3-AB reduced LPS activity by 75% regardless of PJ-34 presence or absence (Fig. 2d). These results imply that 3-AB and PJ-34 inhibit TNF α secretion, at least in part, by distinct mechanisms, and suggest that 3-AB can regulate TNF α expression independently of its activity as a PARP-1 inhibitor.

3-AB Suppresses NF κ B-Dependent Gene Expression

In order to shed light on the mechanism of TNF α secretion inhibition by 3-AB, we initially examined the ability of 3-AB to suppress TNF α transcription by using a TNF α promoter reporter construct. Figure 3a shows that 3-AB was able to inhibit 81% and 86% of LPS-stimulated TNF α promoter activity at 4 h and 24 h, respectively. As NF κ B is the major transcription factor mediating TNF α expression, we also used a luciferase reporter construct regulated by four repeats of the consensus NF κ B recognition sequence. As expected, 3-AB inhibited 86% and 95% of LPS-stimulated NF κ B transcriptional activity at 4 h and 24 h, respectively (Fig. 3b). These results imply that 3-AB inhibits TNF α secretion by suppressing NF κ B transcriptional activity at the TNF α promoter.

The observed inhibition of NF κ B transcriptional activity predicted that 3-AB would also inhibit the NF κ B-regulated gene expression of iNOS, an enzyme catalyzing the production of the important inflammatory mediator nitric oxide (NO). Indeed, 3-AB almost completely abolished iNOS expression (Fig. 4a) and NO production (Fig. 4b) in RAW264.7 macrophages stimulated for 24 h with LPS.

TNF α transcription depends specifically on the p65 subunit of NF κ B [33] whose activation by LPS requires both nuclear translocation and phosphorylation on multiple serine/threonine acceptors [34]. Two well-established activation marks of p65 are Ser-276 and Ser-536 phosphorylation, leading to enhanced transcriptional activity, in part by increasing p65 interaction with the CBP/p300 coactivator and decreasing p65 interaction with corepressors [34]. We set out to determine whether 3-AB affects either of these activation steps. Phosphorylation of p65 on Ser-536 was measured by treatment of RAW264.7 macrophages with LPS and/or 3-AB for the peak time of 30 min, followed by whole-cell lysis and quantitation in western blot. LPS-stimulated p65 phosphorylation by 3.6-fold, while 3-AB did not inhibit, and even modestly increased the phosphorylation (Fig. 5a). Next, we measured NF κ B nuclear translocation and Ser-276 phosphorylation using immuno-fluorescence and high

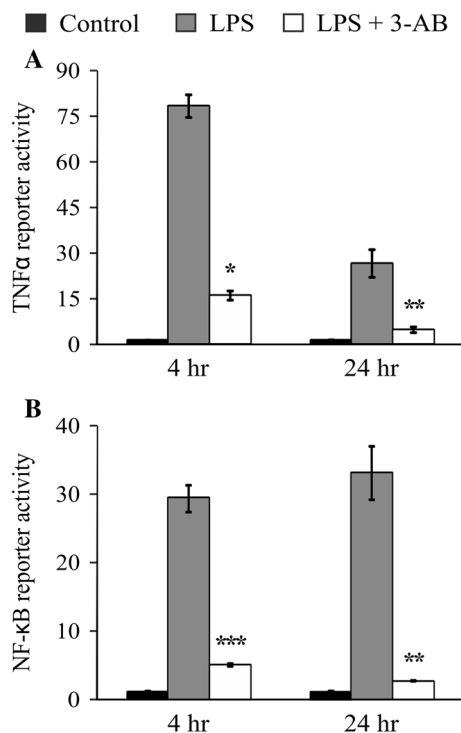


Fig. 3 3-AB inhibits NFκB transcriptional activity and TNFα promoter reporter activity. RAW264.7 macrophages were transfected with a luciferase reporter regulated by the mouse TNFα promoter (a) or by four repeats of a consensus NFκB sequence (b). The cells were pre-incubated with 3-AB (20 mM) or vehicle for 2 h and then LPS (100 ng/ml) was added for the indicated time. Luciferase reporter data expressed as mean \pm SD ($n=3$) of values normalized against Renilla luciferase activity, relative to unstimulated control cells. Values of 3-AB treatment alone were indistinguishable from control values. * $p < 0.05$, ** $p < 0.01$, *** $p < 0.001$

content imaging. LPS sharply increased the nuclear level of phospho-Ser-276 p65 with a peak time of 30 min; surprisingly, 3-AB did not significantly inhibit the effect of LPS (Fig. 5b). In a parallel experiment, we verified that 3-AB inhibited LPS-stimulated TNFα expression as expected (data not shown). Thus, our results indicate that 3-AB does not impair LPS-stimulated p65 nuclear translocation and phosphorylation of Ser-276 and Ser-536, and yet it does abolish NFκB reporter activity.

To verify that 3-AB does not generally inhibit expression of the luciferase reporter, we compared luciferase expression in RAW264.7 cells using three different reporters coding for the firefly luciferase and regulated by either one of the transcription factors—NFκB, AP-1, or CREB. The cells were then stimulated with either LPS—to activate the NFκB- and AP-1-dependent reporters, or with a combination of isoproterenol (a β-adrenergic receptor agonist) and IBMX (a phosphodiesterase inhibitor)—to activate the cAMP-CREB-dependent reporter. Interestingly, 3-AB abolished LPS-stimulated NFκB- and AP-1-dependent

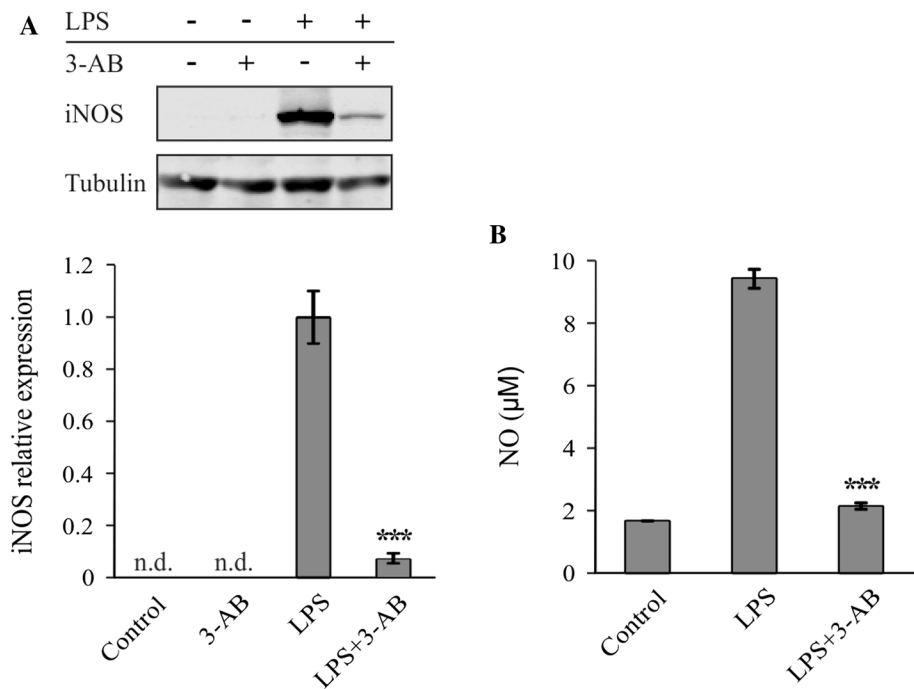
luciferase activity, but had no effect on cAMP-stimulated CREB-dependent luciferase activity (Fig. 5c). These results suggest that 3-AB specifically affects gene expression in pro-inflammatory macrophages and indicate that 3-AB does not generally affect total or luciferase expression.

As 3-AB largely reduced oxidative stress in the ConA-induced mouse liver damage model (Fig. 1b), while reactive oxygen species (ROS) can contribute to TNFα expression [35], we sought to determine whether suppression of NFκB activity and TNFα expression by 3-AB are due to its anti-oxidative activity. To this end, we treated LPS-stimulated macrophages with 3-AB and/or either the well-established ROS scavenger *N*-acetylcysteine (NAC) or diphenyleneiodonium (DPI), an inhibitor of NADPH oxidase (Nox), a key ROS producing enzyme in macrophages [36]. Interestingly, all three compounds significantly inhibited LPS-stimulated TNFα expression and 3-AB demonstrated additivity with either NAC or DPI (Fig. 6a). In contrast, while 3-AB suppressed 90% of NFκB transcriptional activity, NAC inhibited only 45% and DPI even increased NFκB reporter activity by twofold (Fig. 6b). Taken together, these results suggest that 3-AB may inhibit TNFα expression both via NFκB suppression and via an NFκB-independent anti-oxidative mechanism.

3-AB Displays Scavenger Activity for H₂O₂, but Not for the Reactive Superoxide Ion

It was previously suggested that 3-AB serves as a ROS scavenger [37], but detailed information about the exact nature of the ROS involved was lacking. Following stimulation, macrophages respond with an oxidative burst, which was reported to involve Nox creating the highly reactive superoxide ion, from which other ROS, including the more stable H₂O₂, are then derived [36, 38]. To determine whether 3-AB can directly interfere with superoxide production or act as a scavenger for this particular ROS, we employed a cell-free assay, in which the subunits of Nox were reconstituted, NADPH served as a substrate, and superoxide production rate was measured by cytochrome C reduction rate. Figure 7a clearly shows that superoxide formation and level was unaffected by either 3-AB or NAC, whereas it was completely abolished by the pharmacological Nox inhibitor, DPI, as well as by the degrading enzyme, superoxide dismutase (SOD). We then determined whether 3-AB can act as a scavenger for H₂O₂ by pre-incubating H₂O₂ (0.11 μM) with 3-AB at increasing concentrations (1–20 mM) and measuring horseradish peroxidase (HRP) activity. Figure 7b shows that 3-AB efficiently reduced HRP activity with an EC₅₀ of 5.0 \pm 0.5 mM. NAC completely blocked HRP activity (data not shown), but it should be noted that in addition to being a scavenger, NAC also directly interacts with the enzyme [39]. Thus, to conclusively prove that 3-AB indeed

Fig. 4 3-AB inhibits induction of the NF κ B-dependent gene, iNOS. RAW264.7 macrophages were pre-incubated with 3-AB (20 mM) or vehicle for 2 h and then LPS (100 ng/ml) was added for 24 h. **a** iNOS expression was evaluated by WB with tubulin serving for normalization. Data expressed as mean \pm SD ($n=3$); **b** NO level was assessed using the Griess reagent and expressed as mean \pm SD ($n=6$). *** $p < 0.001$



acts as a scavenger for H_2O_2 , we next employed peroxy-fluor-2 (PF2), a highly specific H_2O_2 fluorescent probe [29]. Figure 7c shows that 3-AB scavenged H_2O_2 , albeit with a lower potency ($EC_{50} > 20$ mM) compared to NAC in the same assay ($EC_{50} = 2.0 \pm 0.3$ mM) and also compared to its own activity in the HRP assay (Fig. 7b). The Nox inhibitor DPI had no effect on H_2O_2 detection in either assay (data not shown).

PARP-1 Is Not Required for Inhibition of TNF α Expression by 3-AB

The scavenger activity of 3-AB, together with the TNF α suppression activity of the ROS inhibitors NAC and DPI, promoted us to evaluate whether PARP-1 inhibition by 3-AB is required for its activity as a TNF α suppressor. To that end, PARP-1 expression in RAW264.7 macrophages was down-regulated by siRNA, reaching silencing efficiency of 70% relative to cells transfected with control siRNA (Fig. 8a). Interestingly, 3-AB inhibited LPS-induced TNF α expression to a similar extent in non-transfected control cells and in cells transfected with either siPARP-1 or siControl (Fig. 8b), suggesting that the activity of 3-AB as a PARP-1 inhibitor is not essential for TNF α suppression. Similarly, PARP-1 silencing did not significantly impair the ability of 3-AB to suppress LPS-stimulated NO production (data not shown).

In order to verify that 3-AB activity in the silenced cells is not due to the 30% remaining PARP-1, we generated RAW264.7-derived PARP-1 knockout (PARP-1-KO) macrophages using CRISPR/Cas9 (Fig. 8c). As in the

knockdown experiment, we observed that 3-AB similarly inhibited LPS-induced TNF α secretion in wild-type, mock-transfected, and PARP-1-KO cells (60, 70, and 65%, respectively) (Fig. 8d). Furthermore, 3-AB abolished LPS-stimulated NF κ B transcriptional activity in both wild-type and knockout cells (Fig. 8e). In conclusion, the experiments with PARP-1-KO cells suggest that 3-AB suppresses NF κ B activity and subsequent TNF α expression and secretion by a mechanism which is independent of PARP-1 inhibition.

Discussion

The recent FDA approval of the PARP-1/2 inhibitor olaparib for use in gynecologic oncology [40] may pave the way for its use also in additional indications, including hepatology. The present study was based on the hypothesis that the experimental model of ConA-induced hepatitis might have a pathophysiological similarity with the model of ischemia–reperfusion injury that is characterized by increased activation of PARP-1. This occurs in various circumstances of acute cellular damage, leading to energy crisis and cell necrosis, and therefore, PARP-1 inhibition and/or knockout were widely tested as a potential therapeutic approach. For instance, Biro et al. [41] recently showed that 3-AB markedly attenuated kidney damage in a gentamicin-induced acute tubular necrosis (ATN) rat model. Mukhopadhyay et al. [15] recently demonstrated attenuation of liver injury in the acute and chronic CCl_4 models of liver inflammation and fibrosis by two pharmacologic

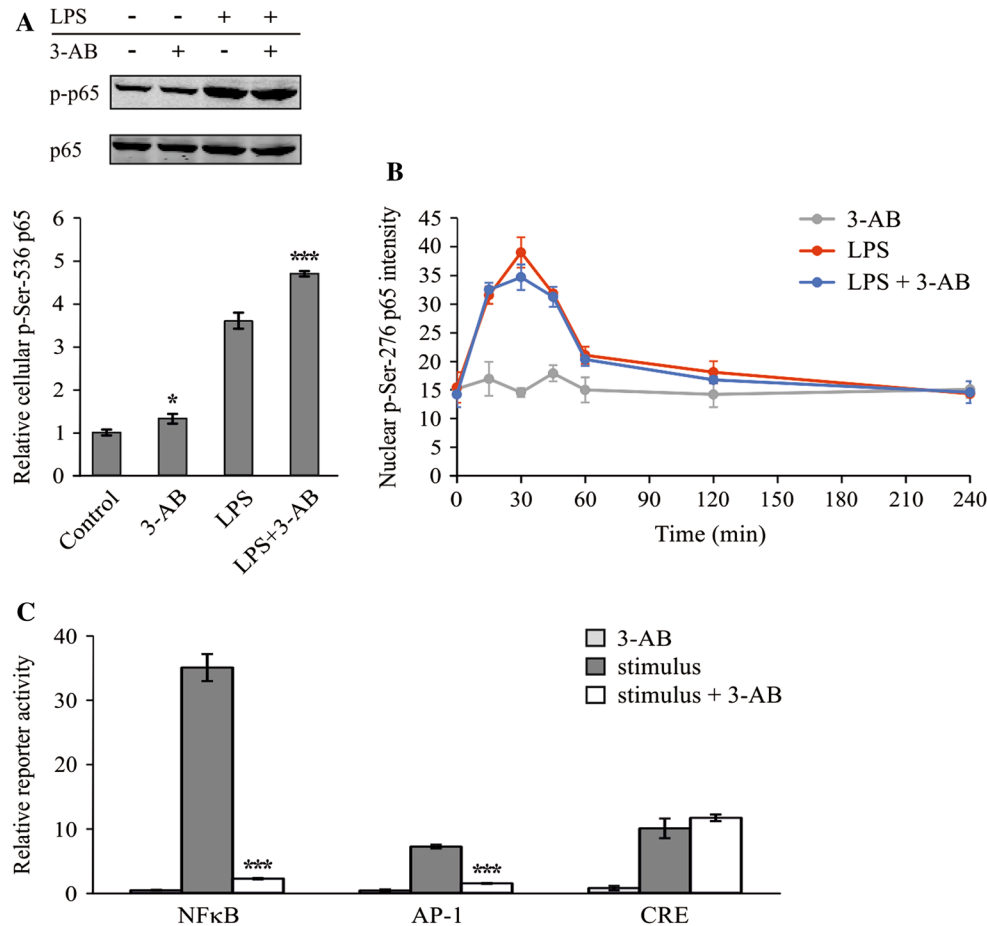


Fig. 5 3-AB does not inhibit NF κ B p65 nuclear translocation and phosphorylation on Ser-276 and Ser-536. **a** RAW264.7 macrophages were pre-incubated with 3-AB (20 mM) or vehicle for 2 h and LPS (100 ng/ml) was added for 30 min. Phosphorylation on Ser-536 of p65 NF κ B was determined by WB of cellular extracts with general p65 NF κ B serving for normalization. Data expressed as mean \pm SD ($n=3$); **b** RAW264.7 macrophages were pre-incubated with 3-AB (20 mM) or vehicle for 2 h and LPS (100 ng/ml) was added for the indicated time. The cells were then fixed, permeabilized, and exposed to phospho-Ser-276 p65 pNF κ B antibody. Data represent mean \pm SD ($n=3$) of fluorescence intensity in 500 nuclei/well (arbitrary units,

divided by 10,000); **c** RAW264.7 macrophages were transfected with a luciferase reporter regulated by four repeats of a consensus NF κ B sequence, five repeats of the AP-1 binding site from the human collagenase promoter, or a CRE-containing EVX-1 promoter. The cells were incubated for 6 h with 3-AB (20 mM) or vehicle in the presence or absence of the relevant stimulus—LPS (100 ng/ml) for the NF κ B and AP-1 reporters or cAMP inducers—*isoproterenol* (1 μ M) and *IBMX* (0.25 mM) for the CRE reporter. Luciferase reporter data expressed as mean \pm SD ($n=3$) of values normalized against Renilla luciferase activity, relative to unstimulated control cells. * $p < 0.05$, *** $p < 0.001$

PARP inhibitors, PJ-34 and AIQ, or by genetic ablation of PARP-1. Thus, in that study, the therapeutic protection provided by PARP-1 knockout apparently confirmed the mechanism of action of the pharmacological inhibitors. However, in other reports, a PARP-1 inhibitor was effective also in the absence of PARP-1 expression, suggesting an off-target effect [42, 43]. The anti-oxidative properties of multiple PARP-1 inhibitors, including 3-AB [37], are likely to play a role, as suggested in the animal model of acetaminophen overdose, where the protective effect of 3-AB largely remained also in PARP-1 knockout mice [42]. Cover et al. [42] further showed that 3-AB inhibits glutathione depletion caused by the reactive metabolite

formed in the liver from acetaminophen (NAPQI) and suggested that 3-AB directly inhibited its formation. However, metabolism of acetaminophen results also in formation of H_2O_2 [44] which can create oxidative stress unless neutralized, for example by glutathione via glutathione peroxidase. Our results suggest that 3-AB inhibits liver damage resulting from administration of ConA, in part by acting as a scavenger for H_2O_2 . This mechanism may be relevant also for acetaminophen cytotoxicity. It should be noted that oxidative stress involves multiple ROS that are generated from H_2O_2 . We show that 3-AB was more potent in inhibiting HRP activity than in reducing the fluorescence of the specific H_2O_2 probe, suggesting that 3-AB may be

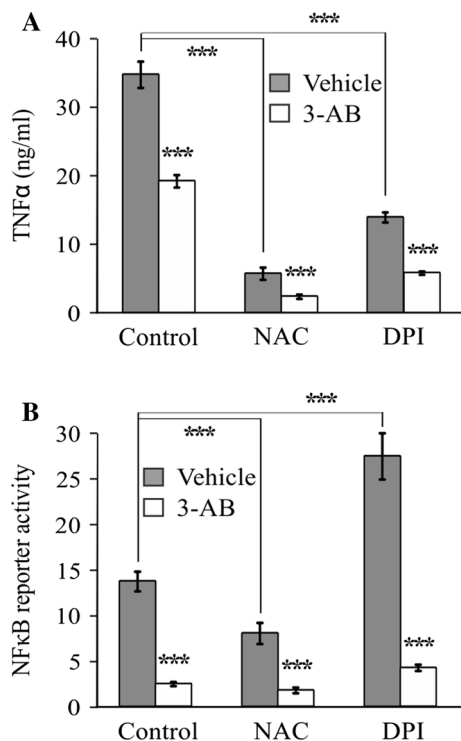


Fig. 6 Oxidative stress inhibitors and 3-AB suppress TNF α expression in an additive manner. RAW264.7 macrophages, transfected with a luciferase reporter regulated by four repeats of a consensus NF κ B sequence, were stimulated for 6 h with LPS (100 ng/ml) in the presence or absence of 3-AB (20 mM) and/or either NAC (20 mM) or DPI (10 μ M). **a** TNF α secretion to the medium was measured by ELISA. Data represent mean \pm SD ($n=6$); **b** Luciferase reporter data expressed as mean \pm SD ($n=6$) of values normalized against Renilla luciferase activity, relative to unstimulated control cells. *** $p < 0.001$

more efficient as a scavenger of ROS derived from H₂O₂ (e.g., hydroxyl radical) compared to H₂O₂ itself [45].

In this study, we show that 3-AB markedly reduced the acute hepatitis and liver necrosis caused by ConA. The reduced oxidative stress may reflect an important mechanism for protection from liver damage by 3-AB, consistent with a previous study showing the efficacy of ROS scavengers in preventing ConA-induced liver damage [21]. Additionally, we show that 3-AB significantly reduced TNF α secretion in the ConA mouse model and in cell culture. This finding suggested that PARP-1 inhibition by 3-AB, resulting in NF κ B suppression [46], is a major mechanism for TNF α suppression by 3-AB. Yet, we also show that anti-oxidative agents, NAC and DPI, strongly inhibit TNF α secretion from macrophages in an NF κ B-independent manner, suggesting that ROS produced in LPS-stimulated macrophages are involved in TNF α secretion. Consistently, LPS-induced ROS are required for expression of TNF α , iNOS, and additional inflammatory factors via the p38 kinase pathway [47]. Thus, the ability of 3-AB to reduce oxidative stress in vivo and to act as a scavenger for H₂O₂ in vitro suggests that the observed inhibition of TNF α and iNOS expression, and subsequent TNF α secretion and NO production may be attributed to dual independent mechanisms—suppression of NF κ B activity and ROS neutralization.

We show that partial PARP-1 silencing or its complete knockout did not significantly impair the ability of 3-AB to inhibit TNF α expression (Fig. 8) or NO production (data not shown). Interestingly, knocking-out PARP-1 did not reverse suppression of NF κ B activity by 3-AB. This result was somewhat surprising in light of previous reports showing that PARP-1 catalyzes poly ADP-ribosylation of the NF κ B p65 subunit, leading to increased nuclear accumulation and activity in LPS-stimulated macrophages [12, 48,

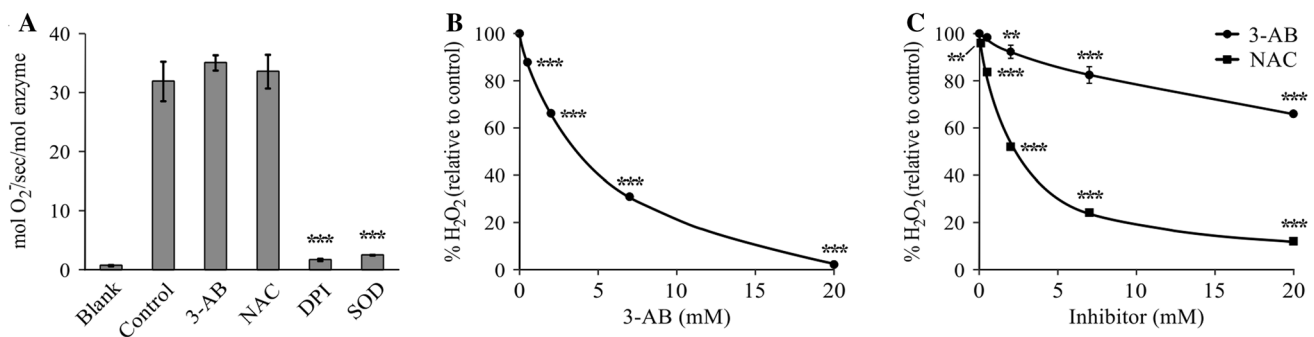
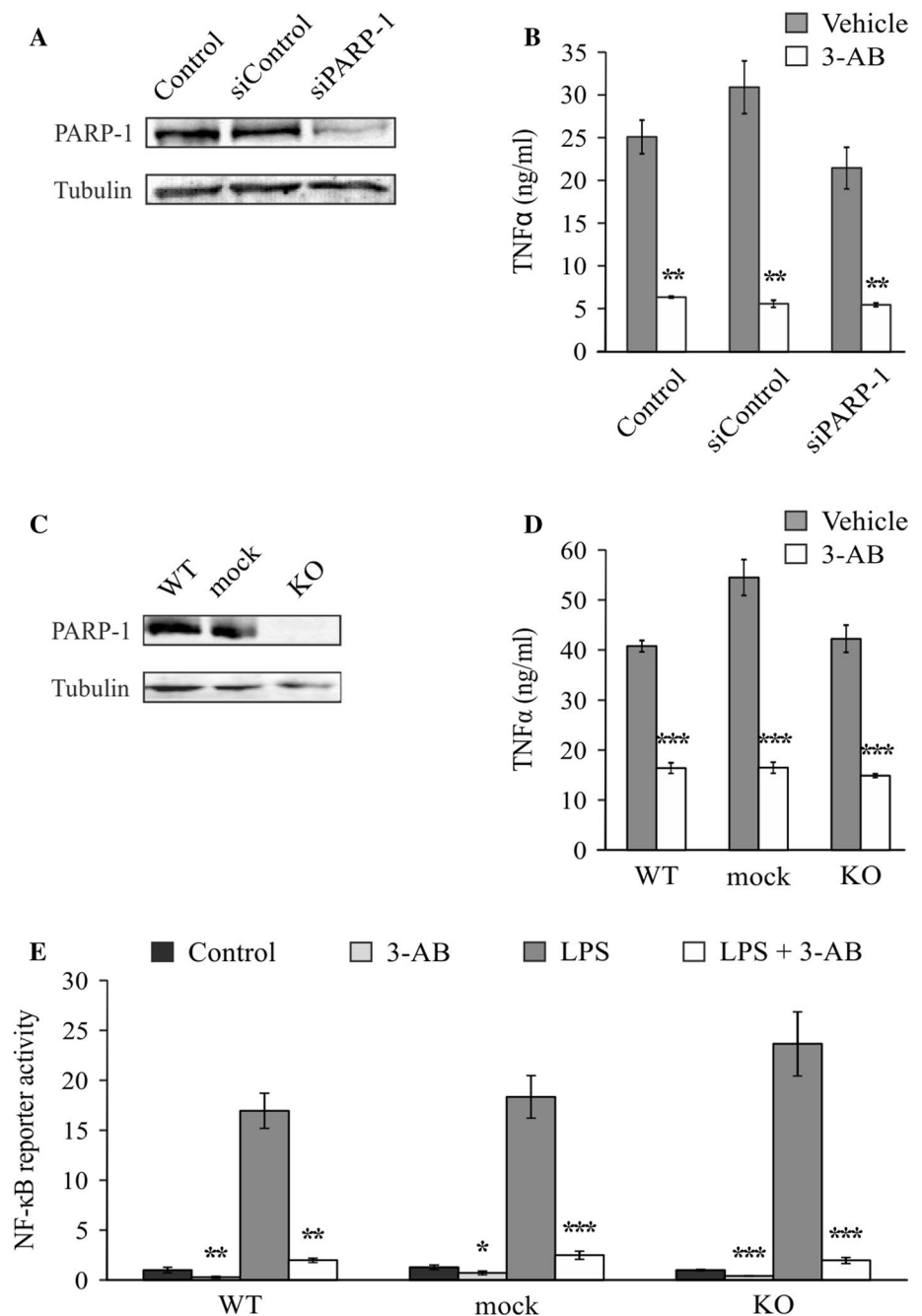


Fig. 7 3-AB acts as a scavenger for H₂O₂, but has no effect on superoxide formation or stability. **a** NADPH was added to a reconstituted cell-free NADPH oxidase complex, and the resulting superoxide was concurrently quantified by a reaction with cytochrome C which then absorbs at 550 nm. Inhibitors tested were 3-AB (10 mM), NAC (20 mM), and DPI (10 μ M) and the enzyme superoxide dismutase (SOD, 250 u/ml). Data represent mean \pm SD of three independent experiments of superoxide formation kinetics (5 min, $n=3$); **b** H₂O₂

(0.22 mM) was mixed with 3-AB (1–20 mM) or vehicle (5% DMSO). HRP-catalyzed oxidation of TMB (0.13 mM) by H₂O₂ was followed for 1.5 min by measurement of the absorbance at 450 nm. Data represent mean \pm SD ($n=3$); **c** H₂O₂ (50 μ M) was mixed with the probe PF2 (0.1 mM) and either 3-AB (0.5–20 mM), NAC (0.1–20 mM) or vehicle (10% DMSO). Fluorescence development at 530 nm was followed for 5 h. Data represent mean \pm SD ($n=3$). ** $p < 0.01$, *** $p < 0.001$

Fig. 8 PARP-1 inhibition is not required for TNF α suppression by 3-AB. **a, b** RAW264.7 macrophages were transfected with siPARP-1 or control siRNA. **a** WB showing 70% silencing efficiency. The blot is representative of 3 independent experiments; **b** the cells were pre-incubated with 3-AB (20 mM) or vehicle for 2 h and then LPS (100 ng/ml) was added for 24 h. TNF α secretion to the medium was measured by ELISA. Data represent mean \pm SD ($n=6$). TNF α was undetectable in resting cells. **c** RAW264.7-derived PARP-1 knockout (KO) cells were generated using CRISPR/Cas9. The WB shows PARP-1 expression in wild-type (WT) RAW264.7 macrophages and in mock-transfected cells, and the complete absence of PARP-1 in the KO cells. **d, e** WT, mock and PARP-1-KO cells were transfected with a luciferase reporter regulated by four repeats of a consensus NF κ B sequence and stimulated for 6 h with LPS (100 ng/ml) in the presence or absence of 3-AB (20 mM). **d** TNF α secretion to the medium was measured by ELISA. Data represent mean \pm SD ($n=4$). TNF α was undetectable in resting cells. **e** Luciferase reporter data expressed as mean \pm SD ($n=4$) of values normalized against Renilla luciferase activity. ** $p < 0.01$, *** $p < 0.001$



49]. It is possible that NF κ B activation by PARP-1 is compensated for by other NAD⁺-binding enzymes which are non-selectively inhibited by 3-AB, including other PARPs and mono-(ADP-ribosyl)transferases [50] or even NADases [51]. Yet, it should be noted that the requirement of PARP-1 expression and/or catalytic activity for NF κ B activation seems to be highly context-dependent rather than a general mechanism [52–54].

We further show that 3-AB neither interferes with nuclear translocation of the NF κ B p65 subunit nor does it interfere with the key activating phosphorylation

events—on Ser-276 and Ser-536 of p65. Although other phosphorylation sites are considered to have a more moderate regulatory effect on p65 activity [34], we cannot exclude the possibility that 3-AB suppresses NF κ B reporter activity by inhibiting phosphorylation on a different p65 site positively associated with transcription, or that it elevates phosphorylation on a p65 site negatively associated with transcription. Alternatively, 3-AB may affect a different posttranslational modification, such as acetylation which has been shown to regulate DNA binding and additional NF κ B functions, or methylation [34].

We verified that 3-AB does not generally inhibit expression of the luciferase reporter. Indeed, 3-AB suppressed NF κ B- and AP-1-dependent reporter activities in LPS-stimulated cells, but not CREB-dependent reporter activity in cells exposed to cAMP inducers. We therefore suggest that the anti-inflammatory effect of 3-AB stems from inhibition of gene expression downstream to TLR4. Rather than a direct effect on the transcription factor, this may result from an effect of 3-AB on regulation by LPS of a component of the transcriptional machinery which is required for the function of both NF κ B and AP-1. For example, in mouse lung epithelial cells, LPS up-regulates the level of the transcriptional coactivator CBP in a time-dependent manner [55].

While the activity of 3-AB as antioxidant appears to be direct and unrelated to its activity as an inhibitor of NF κ B activation, these pathways are known to influence each other. ROS production is upregulated in LPS-stimulated macrophages via NF κ B which stimulates expression of Nox1, while it represses the expression of enzymes that neutralize ROS, such as catalase and glutathione peroxidase [56]. Thus, NF κ B suppression by 3-AB is expected to indirectly augment its direct activity in reducing oxidative stress. This putative cross talk may explain the observed time dependency of TNF α suppression by 3-AB.

Hepatic cell death may occur in various modes, including necrosis, apoptosis, necroptosis, and autophagy, which can exist in parallel. Even a single mode, such as apoptosis, may proceed via distinct and sometimes parallel pathways, depending on the cause of liver injury [57]. Oxidative stress is an integral part of multiple cell death pathways [57–59]. Apart from having a key role in inflammation, TNF α is also able to stimulate apoptosis in hepatocytes [57]. Additionally, ConA-induced liver damage involves TRAIL which is secreted mainly by activated NKT cells and stimulates hepatocyte cell death in a mechanism depending on PARP-1 [60]. Interestingly, while ConA is mainly regarded as a specific T cell activator, it was also reported to directly induce apoptosis of HepG2 cells [61]. Thus, the anti-inflammatory and anti-oxidative activities of 3-AB are expected to reduce external signals for hepatic cell death, and in addition 3-AB is expected also to directly inhibit cell death pathways in hepatocytes due to its activities as a PARP-1 inhibitor and as an antioxidant. Conversely, 3-AB is expected to promote cell death if it abolishes NF κ B activity also in hepatocytes, as shown here for macrophages. This is because NF κ B is generally considered as anti-apoptotic, and its inhibition was demonstrated to be crucial for TNF α -stimulated apoptosis of hepatocytes [62, 63]. Moreover, 3-AB may also promote hepatocyte cell death by inhibiting PARP-1 whose activity can rescue HepG2 cells from oxidative stress-induced apoptosis [59]. It is therefore not surprising that contrasting effects of 3-AB on hepatocyte cell death have been reported [58, 59, 64, 65].

The inflammatory process that leads to liver damage in the ConA mouse model involves immune cells, such as resident macrophages and infiltrating monocytes [3]. These monocytic cells can be activated by cytokines (e.g., TNF α and IFN γ) [4, 5] or short-lived mediators [4] secreted from the ConA-stimulated T cells. Additionally, these cells can be activated via TLR4, either by the pathogen-associated molecular pattern (PAMP) LPS or by danger-associated molecular pattern (DAMP) molecules released from necrotic cells [9, 10]. In fact, TLR4-deficient mice were protected from liver injury in the mouse models of ConA and acetaminophen toxicity [9] and hemorrhagic shock [7]. Thus, the suppressive effect demonstrated here for 3-AB in LPS-stimulated macrophages is highly relevant for its protective effect in the ConA-induced liver damage model.

PARP-1 inhibition was recently demonstrated to attenuate liver injury caused by bile duct ligation [15], CCl₄ [15], acetaminophen overdose [16], and alcohol toxicity [17]. In the current research, we examined the approach of PARP-1 inhibition in the well-described acute immune model of ConA-induced hepatitis that mimics autoimmune hepatitis due to the direct effect of ConA on hepatic T cells, initiating inflammation. Surprisingly, we found that 3-AB suppresses NF κ B activity and inhibits TNF α secretion in macrophages also in the complete absence of PARP-1 expression. Yet, it is possible that PARP-1 inhibition contributes to the overall protective effect of 3-AB in vivo, as PARP-1 activity in hepatocytes is involved in cell death in the ConA model [60], and PARP-1 knockout protects from liver injury in the CCl₄ model [15]. In our study, 3-AB was administered to mice as a preventive treatment. Yet, it is possible that the drug would be efficient also as a therapy following the toxic liver stimulus, as demonstrated for two other PARP-1 inhibitors in the chronic CCl₄ model [15]. The main conclusion derived from our study is that the dual activity of 3-AB as an inhibitor of NF κ B and as a scavenger accounts together for the suppression of TNF α expression and secretion from macrophages, which is manifested in prevention of liver damage in vivo. Thus, our study supports the possibility that a combination of a PARP-1 inhibitor such as olaparib, an NF κ B inhibitor, and an anti-oxidative agent such as NAC might be useful in treatment of acute liver injury of any cause, including cases of acetaminophen overdose which are currently treated by NAC. A single reagent which possesses all these activities, such as 3-AB, may be in particular effective, as shown in this study.

Acknowledgments We are grateful to Dr. C. Daniels and M. Athamna for critical reading of the manuscript, to Dr. M. Cohen-Armon for various reagents and helpful discussions, to Dr. E. Pick and Dr. E. Bechor for the help with the superoxide assay and insightful discussions; to Dr. D. Shabat, N. Hananya and O. Green for help with fluorescence measurement; to Dr. C. Yu (Xiamen University, Xiamen, Fujian, China) for the TNF α promoter luciferase plasmid; to Dr. M. Montminy (Salk

Institute, La-Jolla, CA) for the CRE-luciferase plasmid; to Dr. P. Angel (German Cancer Research Center, Heidelberg, Germany) for the AP-1-luciferase plasmid; to Dr. Ariel Munitz (TAU, Israel) for the iNOS antibody; and to Dr. Y. Ebenstein (TAU, Israel) for the EL-4 cell line.

Author's contribution JW, AB and TZ conceived and designed the study; OE, AL, HA, SK, IBN, IBD, DK, and KR performed the experiments; JW, OE, AL, HA, SK, DK, OB, KR, IF, RW, AB, and TZ analyzed the data; JW, OE, AB, and TZ wrote the manuscript.

Funding This work was supported by the United States – Israel Binational Science Foundation [Grant 2011360 to TZ]. IF is supported by the Intramural Research Program of NIAID, NIH.

Compliance with ethical standards

Conflict of interest The authors declare that they have no conflict of interest.

Ethics approval and consent to participate All animal experiments were performed in accordance with the guidelines of the Care and Use of Laboratory Animals and have been approved by the research ethics committee at Wolfson medical center.

References

- Tiegs G, Hentschel J, Wendel A. A T cell-dependent experimental liver injury in mice inducible by concanavalin A. *J Clin Invest.* 1992;90:196–203.
- Takeda K, Hayakawa Y, Van Kaer L, Matsuda H, Yagita H, Okumura K. Critical contribution of liver natural killer T cells to a murine model of hepatitis. *Proc Natl Acad Sci USA.* 2000;97:5498–5503.
- Schumann J, Wolf D, Pahl A, et al. Importance of Kupffer cells for T-cell-dependent liver injury in mice. *Am J Pathol.* 2000;157:1671–1683.
- Gantner F, Leist M, Kusters S, Vogt K, Volk HD, Tiegs G. T cell stimulus-induced crosstalk between lymphocytes and liver macrophages results in augmented cytokine release. *Exp Cell Res.* 1996;229:137–146.
- Kusters S, Gantner F, Kunstle G, Tiegs G. Interferon gamma plays a critical role in T cell-dependent liver injury in mice initiated by concanavalin A. *Gastroenterology.* 1996;111:462–471.
- Essani NA, Fisher MA, Jaeschke H. Inhibition of NF-kappa B activation by dimethyl sulfoxide correlates with suppression of TNF-alpha formation, reduced ICAM-1 gene transcription, and protection against endotoxin-induced liver injury. *Shock.* 1997;7:90–96.
- Gill R, Tsung A, Billiar T. Linking oxidative stress to inflammation: toll-like receptors. *Free Radic Biol Med.* 2010;48:1121–1132.
- Roh YS, Seki E. Toll-like receptors in alcoholic liver disease, nonalcoholic steatohepatitis and carcinogenesis. *J Gastroenterol Hepatol.* 2013;28:38–42.
- Xu J, Zhang X, Monestier M, Esmon NL, Esmon CT. Extracellular histones are mediators of death through TLR2 and TLR4 in mouse fatal liver injury. *J Immunol.* 2011;187:2626–2631.
- Gong Q, Zhang H, Li JH, et al. High-mobility group box 1 exacerbates concanavalin A-induced hepatic injury in mice. *J Mol Med (Berl).* 2010;88:1289–1298.
- Woodhouse BC, Dianov GL. Poly(ADP-ribose) polymerase-1: an international molecule of mystery. *DNA Repair (Amst).* 2008;7:1077–1086.
- Liu L, Ke Y, Jiang X, et al. Lipopolysaccharide activates ERK-PARP-1-ReIa pathway and promotes nuclear factor-kappaB transcription in murine macrophages. *Hum Immunol.* 2012;73:439–447.
- Huang D, Yang CZ, Yao L, Wang Y, Liao YH, Huang K. Activation and overexpression of PARP-1 in circulating mononuclear cells promote TNF-alpha and IL-6 expression in patients with unstable angina. *Arch Med Res.* 2008;39:775–784.
- Peralta-Leal A, Rodriguez-Vargas JM, Aguilar-Quesada R, et al. PARP inhibitors: new partners in the therapy of cancer and inflammatory diseases. *Free Radic Biol Med.* 2009;47:13–26.
- Mukhopadhyay P, Rajesh M, Cao Z, et al. Poly(ADP-ribose) polymerase-1 is a key mediator of liver inflammation and fibrosis. *Hepatology.* 2014;59:1998–2009.
- Donmez M, Uysal B, Poyrazoglu Y, et al. PARP inhibition prevents acetaminophen-induced liver injury and increases survival rate in rats. *Turk J Med Sci.* 2015;45:18–26.
- Zhang Y, Wang C, Tian Y, et al. Inhibition of poly(ADP-Ribose) polymerase-1 protects chronic alcoholic liver injury. *Am J Pathol.* 2016;186:3117–3130.
- Chen Q, Zhao Y, Cheng Z, Xu Y, Yu C. Establishment of a cell-based assay for examining the expression of tumor necrosis factor alpha (TNF-alpha) gene. *Appl Microbiol Biotechnol.* 2008;80:357–363.
- Conkright MD, Guzman E, Flechner L, Su AI, Hogenesch JB, Montminy M. Genome-wide analysis of CREB target genes reveals a core promoter requirement for cAMP responsiveness. *Mol Cell.* 2003;11:1101–1108.
- Angel P, Karin M. The role of Jun, Fos and the AP-1 complex in cell-proliferation and transformation. *Biochim Biophys Acta.* 1991;1072:129–157.
- Shirin H, Aeed H, Alin A, et al. Inhibition of immune-mediated concanavalin a-induced liver damage by free-radical scavengers. *Dig Dis Sci.* 2010;55:268–275.
- Wills ED. Lipid peroxide formation in microsomes. General considerations. *Biochem J.* 1969;113:315–324.
- Batts KP, Ludwig J. Chronic hepatitis. An update on terminology and reporting. *Am J Surg Pathol.* 1995;19:1409–1417.
- Fraser I, Liu W, Rebres R, et al. The use of RNA interference to analyze protein phosphatase function in mammalian cells. *Methods Mol Biol.* 2007;365:261–286.
- Ran FA, Hsu PD, Wright J, Agarwala V, Scott DA, Zhang F. Genome engineering using the CRISPR-Cas9 system. *Nat Protoc.* 2013;8:2281–2308.
- Cong L, Ran FA, Cox D, et al. Multiplex genome engineering using CRISPR/Cas systems. *Science.* 2013;339:819–823.
- Ernst O, Vayttaden SJ, Fraser IDC. Measurement of NF-kappaB activation in TLR-activated macrophages. *Methods Mol Biol.* 2018;1714:67–78.
- Pick E. Cell-free NADPH oxidase activation assays: “in vitro veritas”. *Methods Mol Biol.* 2014;1124:339–403.
- Dickinson BC, Huynh C, Chang CJ. A palette of fluorescent probes with varying emission colors for imaging hydrogen peroxide signaling in living cells. *J Am Chem Soc.* 2010;132:5906–5915.
- Ernst O, Zor T. Linearization of the Bradford protein assay. *J Vis Exp.* 2010;38:e1918.
- Zor T, Selinger Z. Linearization of the Bradford protein assay increases its sensitivity: theoretical and experimental studies. *Anal Biochem.* 1996;236:302–308.
- Hatano M, Sasaki S, Ohata S, et al. Effects of Kupffer cell-depletion on concanavalin A-induced hepatitis. *Cell Immunol.* 2008;251:25–30.
- Koga K, Takaesu G, Yoshida R, et al. Cyclic adenosine monophosphate suppresses the transcription of proinflammatory cytokines via the phosphorylated c-Fos protein. *Immunity.* 2009;30:372–383.

34. Huang B, Yang XD, Lamb A, Chen LF. Posttranslational modifications of NF-kappaB: another layer of regulation for NF-kappaB signaling pathway. *Cell Signal*. 2010;22:1282–1290.
35. Mills EL, O'Neill LA. Reprogramming mitochondrial metabolism in macrophages as an anti-inflammatory signal. *Eur J Immunol*. 2016;46:13–21.
36. Forman HJ, Torres M. Reactive oxygen species and cell signaling: respiratory burst in macrophage signaling. *Am J Respir Crit Care Med*. 2002;166:S4–S8.
37. Czapski GA, Cakala M, Kopczuk D, Strosznajder JB. Effect of poly(ADP-ribose) polymerase inhibitors on oxidative stress evoked hydroxyl radical level and macromolecules oxidation in cell free system of rat brain cortex. *Neurosci Lett*. 2004;356:45–48.
38. Pick E, Keisari Y. Superoxide anion and hydrogen peroxide production by chemically elicited peritoneal macrophages—induction by multiple nonphagocytic stimuli. *Cell Immunol*. 1981;59:301–318.
39. Aruoma OI, Halliwell B, Hoey BM, Butler J. The antioxidant action of *N*-acetylcysteine: its reaction with hydrogen peroxide, hydroxyl radical, superoxide, and hypochlorous acid. *Free Radic Biol Med*. 1989;6:593–597.
40. Scott CL, Swisher EM, Kaufmann SH. Poly(ADP-ribose) polymerase inhibitors: recent advances and future development. *J Clin Oncol*. 2015;33:1397–1406.
41. Biro A, Vaknine H, Cohen-Armon M, et al. The effect of poly(ADP-ribose) polymerase inhibition on aminoglycoside-induced acute tubular necrosis in rats. *Clin Nephrol*. 2016;85:226–234.
42. Cover C, Fickert P, Knight TR, et al. Pathophysiological role of poly(ADP-ribose) polymerase (PARP) activation during acetaminophen-induced liver cell necrosis in mice. *Toxicol Sci*. 2005;84:201–208.
43. Lakatos P, Szabo E, Hegedus C, et al. 3-Aminobenzamide protects primary human keratinocytes from UV-induced cell death by a poly(ADP-ribosylation) independent mechanism. *Biochim Biophys Acta*. 2013;1833:743–751.
44. Jamil I, Symonds A, Lynch S, Alalami O, Smyth M, Martin J. Divergent effects of paracetamol on reactive oxygen intermediate and reactive nitrogen intermediate production by U937 cells. *Int J Mol Med*. 1999;4:309–312.
45. Mittal M, Siddiqui MR, Tran K, Reddy SP, Malik AB. Reactive oxygen species in inflammation and tissue injury. *Antioxid Redox Signal*. 2014;20:1126–1167.
46. Abd Elmageed ZY, Naura AS, Errami Y, Zerfaoui M. The poly(ADP-ribose) polymerases (PARPs): new roles in intracellular transport. *Cell Signal*. 2012;24:1–8.
47. Matsuzawa A, Saegusa K, Noguchi T, et al. ROS-dependent activation of the TRAF6-ASK1-p38 pathway is selectively required for TLR4-mediated innate immunity. *Nat Immunol*. 2005;6:587–592.
48. Le Page C, Sanceau J, Drapier JC, Wietzerbin J. Inhibitors of ADP-ribosylation impair inducible nitric oxide synthase gene transcription through inhibition of NF kappa B activation. *Biochem Biophys Res Commun*. 1998;243:451–457.
49. Zerfaoui M, Errami Y, Naura AS, et al. Poly(ADP-ribose) polymerase-1 is a determining factor in Crm1-mediated nuclear export and retention of p65 NF-kappa B upon TLR4 stimulation. *J Immunol*. 2010;185:1894–1902.
50. Hassa PO, Hottiger MO. The functional role of poly(ADP-ribose) polymerase 1 as novel coactivator of NF-kappaB in inflammatory disorders. *Cell Mol Life Sci*. 2002;59:1534–1553.
51. Masmoudi A, Mandel P. ADP-ribosyl transferase and NAD glycohydrolase activities in rat liver mitochondria. *Biochemistry*. 1987;26:1965–1969.
52. Ha HC, Hester LD, Snyder SH. Poly(ADP-ribose) polymerase-1 dependence of stress-induced transcription factors and associated gene expression in glia. *Proc Natl Acad Sci USA*. 2002;99:3270–3275.
53. Hassa PO, Haenni SS, Buerki C, et al. Acetylation of poly(ADP-ribose) polymerase-1 by p300/CREB-binding protein regulates coactivation of NF-kappaB-dependent transcription. *J Biol Chem*. 2005;280:40450–40464.
54. Oliver FJ, Menissier-de Murcia J, Nacci C, et al. Resistance to endotoxic shock as a consequence of defective NF-kappaB activation in poly(ADP-ribose) polymerase-1 deficient mice. *EMBO J*. 1999;18:4446–4454.
55. Wei J, Dong S, Bowser RK, et al. Regulation of the ubiquitylation and deubiquitylation of CREB-binding protein modulates histone acetylation and lung inflammation. *Sci Signal*. 2017;10:eaak9660.
56. Menon D, Coll R, O'Neill LA, Board PG. Glutathione transferase omega 1 is required for the lipopolysaccharide-stimulated induction of NADPH oxidase 1 and the production of reactive oxygen species in macrophages. *Free Radic Biol Med*. 2014;73:318–327.
57. Wang K. Molecular mechanisms of hepatic apoptosis. *Cell Death Dis*. 2014;5:e996.
58. Kanno S, Ishikawa M, Takayanagi M, Takayanagi Y, Sasaki K. Characterization of hydrogen peroxide-induced apoptosis in mouse primary cultured hepatocytes. *Biol Pharm Bull*. 2000;23:37–42.
59. Shin SM, Cho IJ, Kim SG. Resveratrol protects mitochondria against oxidative stress through AMP-activated protein kinase-mediated glycogen synthase kinase-3beta inhibition downstream of poly(ADP-ribose)polymerase-LKB1 pathway. *Mol Pharmacol*. 2009;76:884–895.
60. Jouan-Lanhouet S, Arshad MI, Piquet-Pellorce C, et al. TRAIL induces necroptosis involving RIPK1/RIPK3-dependent PARP-1 activation. *Cell Death Differ*. 2012;19:2003–2014.
61. Liu Z, Li X, Ding X, Yang Y. In silico and experimental studies of concanavalin A: insights into its antiproliferative activity and apoptotic mechanism. *Appl Biochem Biotechnol*. 2010;162:134–145.
62. Imose M, Nagaki M, Naiki T, et al. Inhibition of nuclear factor kappaB and phosphatidylinositol 3-kinase/Akt is essential for massive hepatocyte apoptosis induced by tumor necrosis factor alpha in mice. *Liver Int*. 2003;23:386–396.
63. Wang K. Molecular mechanisms of hepatic apoptosis regulated by nuclear factors. *Cell Signal*. 2015;27:729–738.
64. Kanno S, Ishikawa M, Takayanagi M, Takayanagi Y, Sasaki K. Combination acetaminophen and doxapram potentiated hepatotoxicity in mouse primary cultured hepatocytes. *Methods Find Exp Clin Pharmacol*. 1999;21:647–652.
65. Shen W, Kamendulis LM, Ray SD, Corcoran GB. Acetaminophen-induced cytotoxicity in cultured mouse hepatocytes: effects of Ca(2+)-endonuclease, DNA repair, and glutathione depletion inhibitors on DNA fragmentation and cell death. *Toxicol Appl Pharmacol*. 1992;112:32–40.

Affiliations

Joram Wardi¹ · Orna Ernst^{2,3} · Anna Lilja² · Hussein Aeed¹ · Sebastián Katz² · Idan Ben-Nachum² · Iris Ben-Dror² · Dolev Katz² · Olga Bernadsky⁴ · Rajendar Kandhikonda⁵ · Yona Avni¹ · Iain D. C. Fraser³ · Roy Weinstein⁵ · Alexander Biro⁶ · Tsaffrir Zor² 

Orna Ernst
ornaernst@gmail.com

Anna Lilja
anna.lilja88@gmail.com

Hussein Aeed
haeed@wolfson.health.gov.il

Sebastián Katz
seba120777@gmail.com

Idan Ben-Nachum
nachum1989@gmail.com

Iris Ben-Dror
irisbend@tauex.tau.ac.il

Dolev Katz
katz.dolev@gmail.com

Olga Bernadsky
olgabe@wolfson.health.gov.il

Rajendar Kandhikonda
rajendarcdri@gmail.com

Yona Avni
avni@wolfson.health.gov.il

Iain D. C. Fraser
fraseri@niaid.nih.gov

Roy Weinstein
royweinstein@post.tau.ac.il

¹ Department of Gastroenterology, E. Wolfson Medical Center, P.O.B. 5, 58100 Holon, Israel

² Department of Biochemistry and Molecular Biology, Life Sciences Faculty, Tel-Aviv University, 69978 Tel-Aviv, Israel

³ Signaling Systems Section, Laboratory of Immune System Biology, National Institute of Allergy and Infectious Diseases, National Institutes of Health, Bethesda, MD 20892, USA

⁴ Department of Pathology, E. Wolfson Medical Center, P.O.B. 5, 58100 Holon, Israel

⁵ Department of Molecular Biology and Ecology of Plants, Life Sciences Faculty, Tel-Aviv University, 69978 Tel-Aviv, Israel

⁶ Institute of Nephrology, E. Wolfson Medical Center, P.O.B. 5, 58100 Holon, Israel